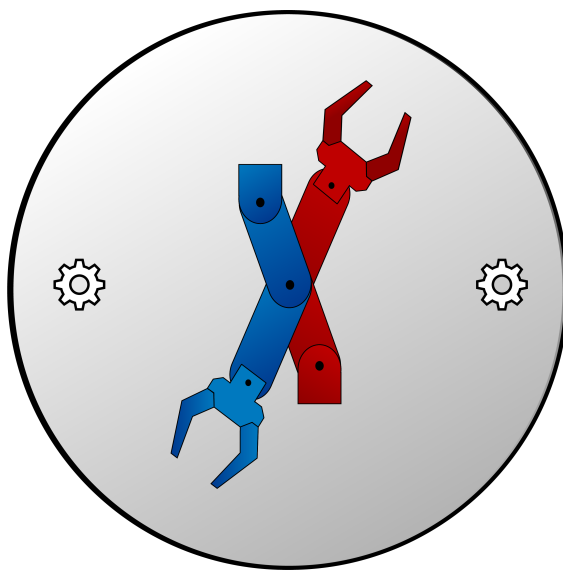


FINAL REPORT

Trey Dufrene, Alan Wallingford, David Orcutt, Ryan Warner, Zack Johnson



ME 407

Preliminary Design of Robotic Systems

Embry-Riddle Aeronautical University



Meiosis

Contents

1	Introduction	1
2	Requirements	1
3	Conceptual Design	3
	3.3 Electrical	6
4	Specifications	8
5	Preliminary Design	13
	5.1 CAD	13
	5.2 Forward Kinematics	14
	5.3 Velocity Kinematics	16
	5.4 Inverse Kinematics	16
	5.5 Equations of Motion	17
	5.6 Open-Loop Simulation	18
	5.7 Control System	18
	5.8 Closed-Loop Simulation	19
	5.9 ANSYS	22
	5.10 Electrical Schematic	22
	5.11 Software Flowchart	22
	5.12 Project Status and Future	22
	5.13 Parts List	22

List of Figures

1	Overall System Conceptual Design	3
2	Manipulator Base with Call-outs	4
3	Drawing Showing Key Features of Design	5
4	Drawing Showing Link Cross Section	5
5	Electrical System Block Diagram	6
6	Software Flowchart	7
7	Overview of Physical System	8
8	Elbow Manipulator Configuration with Link Offset	9
9	Kinematic Model Representing Zeroed Configuration	11
10	Pulley 1-2 Center Distance	13
11	Pulley 3 Center Distance	13
12	Coordinate Systems	14
13	Joint Angles vs Time	21
14	Cross Section of Dexterous Workspace Quadrant	24

List Of Acronyms and Abbreviations

- FK Forward Kinematics
- IK Inverse Kinematics
- PD Proportional Derivative

Notation

$r_{\text{From Frame To}}$ Direction Vectors

$T_{\text{From To}}$ Direction Cosine (Transformation) Matrices

$$c_{\theta_{nm}} \quad \cos(\theta_n + \theta_m)$$

$$s_{\theta_{nm}} \quad \sin(\theta_n + \theta_m)$$

1 Introduction

2 Requirements

Robotics is a fast growing field, yet numerous potential innovators for the discipline are never exposed to it. While many industrial style manipulators are available for commercial applications, their cost is so high that they are not practical for many educational purposes. Schools in rural areas are financially limited and cannot afford a manipulator, nor an instructor who can teach the course due to its complexity. Hence, we propose MEIOSIS robotics: The Manipulator for Educational Institutions with Open Source Integrated Systems. The goal of the project is to produce an inexpensive, rudimentary but capable manipulator that can be purchased as a kit by educators but is available to the general public.

2.1 Design Requirements

In order to create a manipulator that solves the problem stated above, the following requirements must be met.

2.2 Hardware

The following requirements are hardware specific and dictate the physical constraints the system must adhere to.

2.2.1 The system shall cost the end-user no more than \$1000.

2.2.2 The system shall be fully dexterous without being kinematically redundant.

To create a system with the intention of advancing education, it must be complex enough to encourage higher level problem solving, as well as be capable enough (dexterous) in a broad spectrum of tasks — in the interest of remaining useful in addition to retaining the interest of students.

2.2.3 The system end effector shall maintain a positional accuracy magnitude of ± 1 mm and an orientation accuracy of $\pm 5^\circ$ eigen angle from the base frame.

To ensure that the robot has educational value, the accuracy must be defined so that any desired positions and movements are achieved.

- 2.2.4 The system end effector shall maintain a pose repeatability magnitude between 0.1—1.5 mm for the position and $\pm 4^\circ$ eigen angle from the base frame for the orientation.**

This is to ensure a robot that can execute the same movement commands repeatedly and have the same results every time.

- 2.2.5 The system's reachable workspace shall be a hemisphere with a radius of 300-700 mm.**

This workspace will provide enough movement to manipulate objects in order to perform basic tasks.

- 2.2.6 The system's dexterous workspace shall contain a hemispherical shell within the reachable workspace with a thickness of 280 mm.**

- 2.2.7 The system shall have a removable end effector capable of picking and placing a low-odor chisel tip Expo dry erase marker.**

This creates a robot capable of performing a variety of basic tasks, which enhances its educational value.

- 2.2.8 The system shall be able to write with a low-odor chisel tip Expo dry erase marker.**

2.3 Software

- 2.3.1 The system shall be open source.**

This will create an easily obtainable, low cost method of distributing the system's source code, which may be modified for personal use.

- 2.3.2 The system shall be capable of operating given only desired end effector cartesian coordinates specified with respect to the base frame.**

This simplicity makes the system of use to inexperienced users.

3 Conceptual Design

The terminator T-2000 is a science-fiction spectacle of a robot – until you see the price. Channeling the inspiration many high school students may have for robotics, MEIOSIS robotics aims to provide an affordable manipulator to educators and enthusiasts. MEIOSIS uses primarily 3-D printed components and easily accessible materials. Among these materials are a Raspberry PI, smart servos and metal tubing. These features create an open-source manipulator accessible to the public to further robotics education.

3.1 Physical System Overview

The physical design of the robotic manipulator will be shown through Figures 1, 2, 3, and 4.

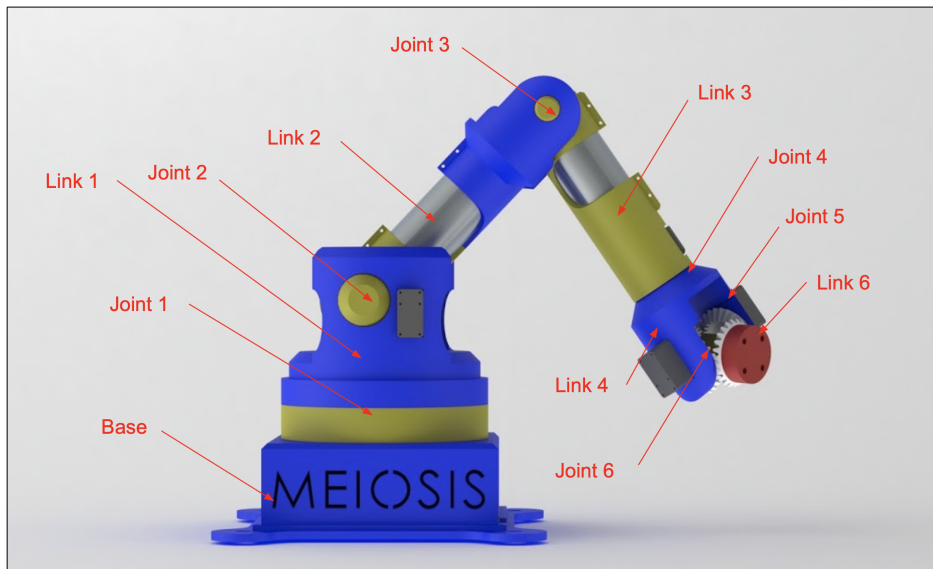


Figure 1: Overall System Conceptual Design

The colored links in *Figure 1* distinguish the different joints and links of the manipulator. The overall reach of the robot will be 582.5 mm. This length was chosen to decrease material cost and weight while still satisfying requirement 2.1.2 and 2.1.5, allowing the manipulating to pick and place objects to perform basic tasks. The base of the robot will be made to contain the Raspberry Pi and other electrical components.

3.1.1 Base

The base of the manipulator will house several of the electronic components, such as the computational system, power supply, and motor controller. A cross section of the base can be seen in *Figure 2*.

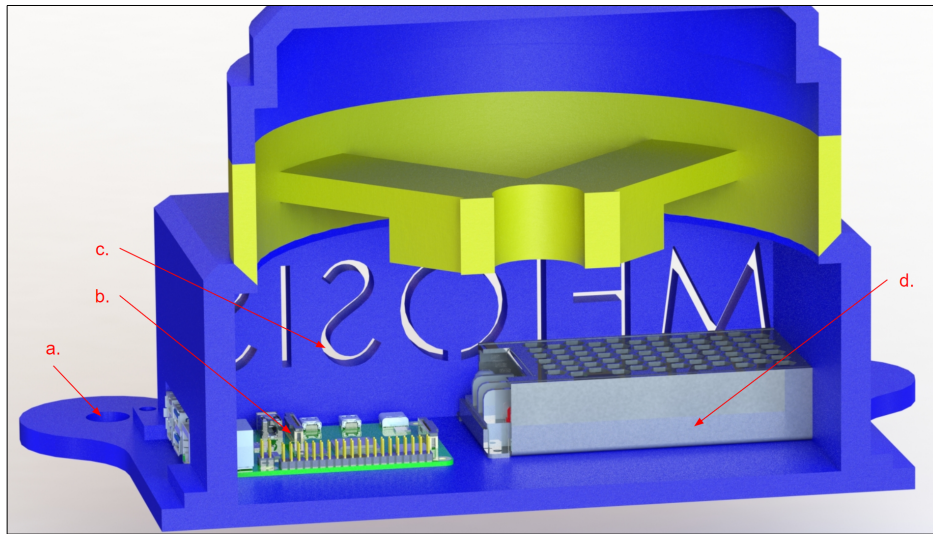


Figure 2: Manipulator Base with Call-outs

From *Figure 2*,

- a. *Base Supports*: The base supports are located at each corner of the base and will allow the base of the manipulator to be securely attached to a variety of surfaces with either standard bolt/fastener hardware or suction cups.
- b. *Computational System*: The computational system will be a Raspberry Pi; it will be housed in the base, which allows the Raspberry Pi to be more easily accessible. The primary reason for this system being chosen is to fulfill the budget requirement, 2.1.1. The Raspberry Pi will compute the manipulator's kinematics and command the motors accordingly.
- c. *Airflow Cutouts*: The side of the base will have cutouts to allow for airflow through the base; since the power supply is housed inside of the base as well as the computational system, the temperature must be regulated to prevent overheating.
- d. *Power Supply*: The power supply will be housed in the base as well; this allows the power supply to be more accessible and therefore more modifiable, so the end-user can easily expand the system to fulfill their needs.

3.1.2 Links

Figure 3 is an image of the robot that shows the links and their key features.

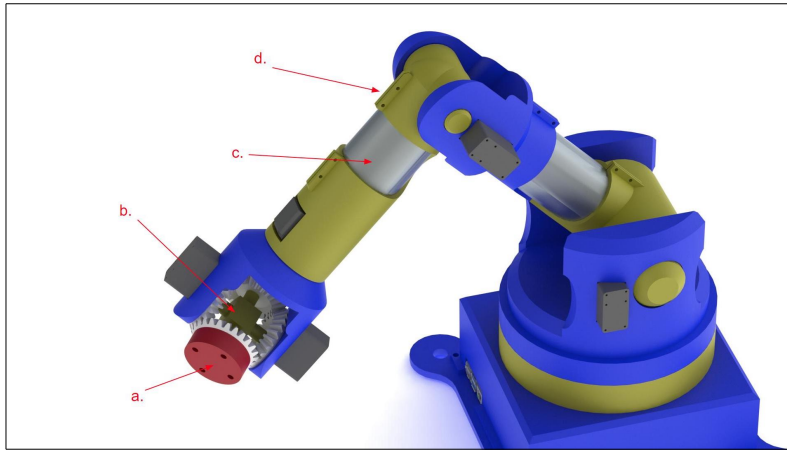


Figure 3: Drawing Showing Key Features of Design

Figure 3 highlights a few of the key features of our design. Call-out a shows the connection point for the end effector. The mountings are the standard used by the Sawyer manipulator. This may be adjusted to accommodate lower cost, more accessible end effectors. Call-out (b) shows the differential gearbox that will be used in the manipulator's wrist, saving space and weight. The manipulator will have aluminum tubing as support in the links (c) and will be attached to the 3D printed portion of the robot using clamp joints (d) tightened by screws.

Figure 4 is an image of the cross section of link 2 for the manipulator.

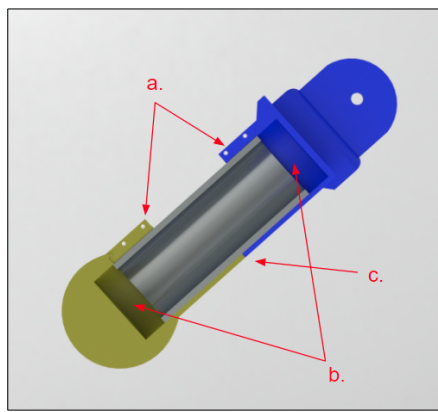


Figure 4: Drawing Showing Link Cross Section

The cross section seen in *Figure 4* shows the internal design for links two and three. It features two clamps that hold a hollow aluminum bar in place (a) and allows for gaps between the

aluminum tube and the 3D printed call-out (b). The proper length will be dictated by the 3D printed guides lining up at call-out (c). This allows for imprecision in the manufacturing of the aluminum tube.

3.2 System Functions

The system can be divided into two subsystems: the electrical and software systems. The electrical subsystem includes the wiring and hardware computational components, power system, actuators with drivers, and sensors. The software subsystem includes the algorithm for the computational system.

3.3 Electrical

Figure 5 is the block diagram for the electrical system of the manipulator.

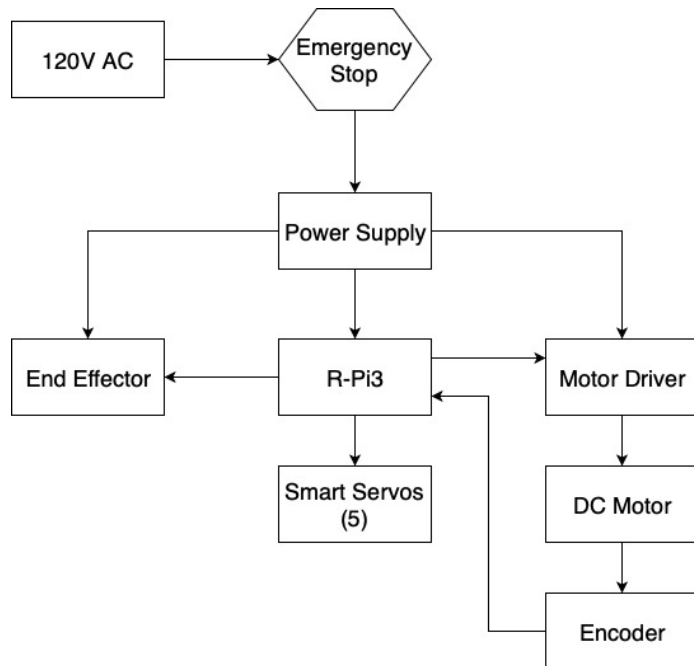


Figure 5: Electrical System Block Diagram

Figure 5 shows that the electrical systems of the manipulator will be relatively simple. Power is supplied by the 120V AC from standard wall outlets. A power supply will adapt the AC voltage to the required voltages for each component. One component is the Raspberry Pi, which will perform calculations for motor control (described below in software). It will send signals to the DC motor driver and the five smart servos. The smart servos have an on-board controller, so no feedback will be necessary. However, the first joint, between the base and the first link, will be actuated by a DC motor with an encoder to minimize cost.

3.4 Software

Figure 6 shows the software flowchart for the system.

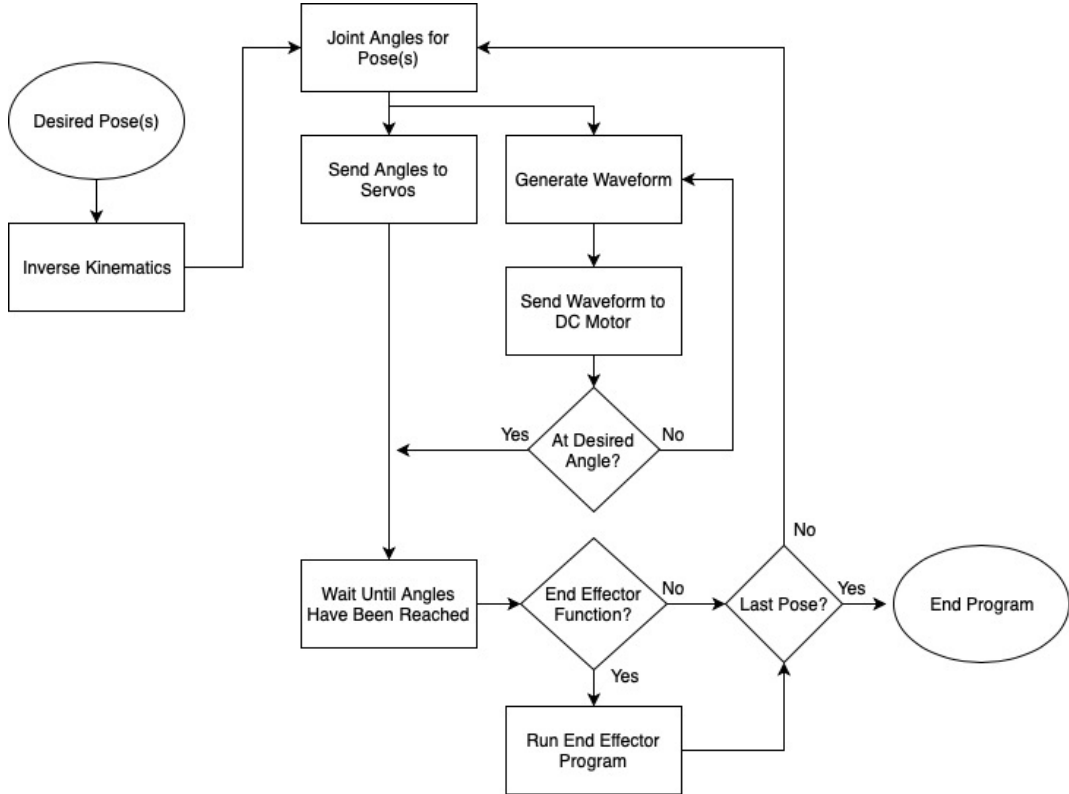


Figure 6: Software Flowchart

Similar to the electrical system, the software is also simple. *Figure 6* shows that the software will receive the desired pose or poses the user would like the manipulator to reach. Then the Raspberry Pi will use inverse kinematics to calculate the necessary joint angles. The waveforms/desired angles will be sent to the respective drivers/motors, and positional information will be sent back to the Raspberry Pi to adjust the DC motor angle. When the motors have reached their desired pose, the Raspberry Pi will actuate the end effector if it is specified by the user. The system will then check to see if there are any more poses to reach and either repeat the motor control section given the desired angles of the new pose or end program if the last pose has been reached.

4 Specifications

With the intention of making robotics education more accessible, The Manipulator for Educational Institutions with Open Source Integrated Systems (MEIOSIS) intends to provide high school educators and robot enthusiasts with a low cost manipulator. The system should be usable by novice students. It should also be modifiable to create a sustainably increased understanding of robotics. While MEIOSIS may not fully emulate industrial manipulators, it aims to provide more students with access to robotics education.

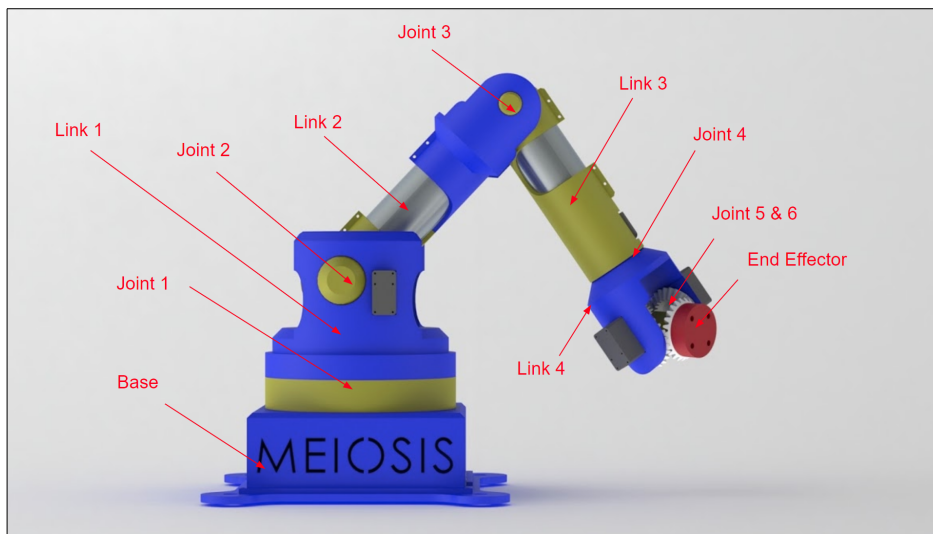


Figure 7: Overview of Physical System

The design seen in *Figure 7* is based on our conceptual design. It features four links and six joints for rotation and will be referenced throughout this document. The base of the manipulator and end-effector can also be seen in the figure.

4.1 Design Requirements

The specifications of the system are strictly based on the requirements defined previously. The requirements are divided into two primary categories, hardware and software.

4.2 Hardware

The following requirements and specifications are hardware specific and dictate the physical constraints the system must adhere to.

4.2.1 The system shall cost the end-user no more than \$1000.

4.2.1.a *The cost for the MEIOSIS team to develop the manipulator shall cost no more than \$800.*

4.2.2 The system shall be fully dexterous without being kinematically redundant.

4.2.2.a The system shall consist of six rotational joints connected by four links. The last three joints will create a spherical wrist.

As defined [1], “A manipulator having more than six DOF is referred to as a kinematically redundant manipulator (5).” A manipulator with less than six degrees of freedom will not be fully dexterous within it’s workspace. *Figure 9* (see subsection 4.2.6, p. 11) shows a six degree-of-freedom rotary manipulator with it’s coordinate frames in zeroed positions. The joint and link locations are seen in *Figure 7* (see section 4, p. 8).

4.2.2.b The system shall have no link offsets.

Link offsets as seen in *Figure 8* are commonly used to avoid singularities. However, having a link offset prevents the manipulator’s dexterous workspace from being a complete hemispherical shell.

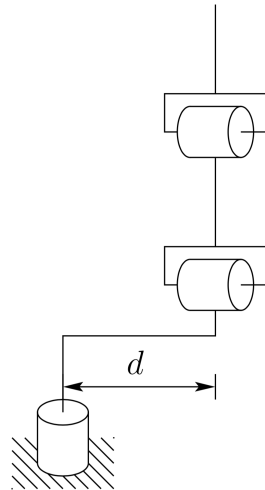


Figure 8: Elbow Manipulator Configuration with Link Offset [1]

As shown in *Figure 8*, the line directly above the first joint of the manipulator is offset such that the axes of the other joints are unable to become collinear with the base axis; this prevents singularity but causes a void in the dexterous workspace.

4.2.3 The system end effector shall maintain a positional accuracy magnitude of ± 1 mm and an orientation accuracy of $\pm 5^\circ$ eigen angle from the base frame.

To ensure that the robot has educational value, the accuracy must be defined so that any desired positions and movements are achieved.

4.2.3.a The system shall accommodate a process in which the end user can calibrate the end effector position and orientation to within 0.5 mm and 1 degree of the manipulator's precision.

The addition of a calibration process allows the removal of any systematic errors, such as drift. The theoretical limit of the calibration process is the difference between the precision and accuracy metrics of the system.

4.2.4 The system end effector shall maintain a pose repeatability magnitude between 0.1—1.5 mm for the position and $\pm 4^\circ$ eigen angle from the base frame for the orientation.

4.2.4.a Joint one and two of the system shall possess an angle error of no more than .025 degrees.

Being that joint one and two are the first two rotational elements in the system, their error will propagate the most to the end effector's position.

4.2.4.b Joint three of the system shall possess an angle error of no more than .03 degrees.

Since joint three is closer to the end effector it's error will not propagate as severely throughout the system.

4.2.4.c Joints four, five, and six shall possess an angle error of no more than .29 degrees.

The spherical wrist is the closest to the end effector's final position and therefore has the least error propagation.

4.2.5 The system's reachable workspace shall be a hemisphere with a radius of 300-700 mm.

This workspace will provide enough movement to manipulate objects in order to perform basic tasks.

4.2.5.a The length of link one, two, three, four, and the wrist shall be 220.8 mm, 250 mm, 200 mm, 80 mm, and 52.5 mm respectively.

This results in a total height of 220.8 mm with a total reach of 582.5 mm in the zeroed configuration as shown in the configuration represented in *Figure 9*.

4.2.6 The system's dexterous workspace shall contain a hemispherical shell within the reachable workspace with a thickness of 280 mm.

This workspace will provide enough movement to manipulate objects in order to perform basic tasks. 280mm is slightly greater than the length of letter paper.

4.2.6.a The rotational limit of joint one, two, three, four, five, and six shall be $\pm 180^\circ$, -9.7° to 177.5° , -150.6° to -19.3° , $\pm 180^\circ$, -180° to -1.6° , and $\pm 180^\circ$ respectively.

The angles stated are with respect to the kinematic model shown in *Figure 9*. To be fully dexterous within our 280 mm dexterous workspace the manipulator must have the joint angles specified above. The joint limitations were calculated by iteratively verifying the orientation about every point within the quarter hemisphere cross section seen in *Figure 14* (see Appendix, p. 24).

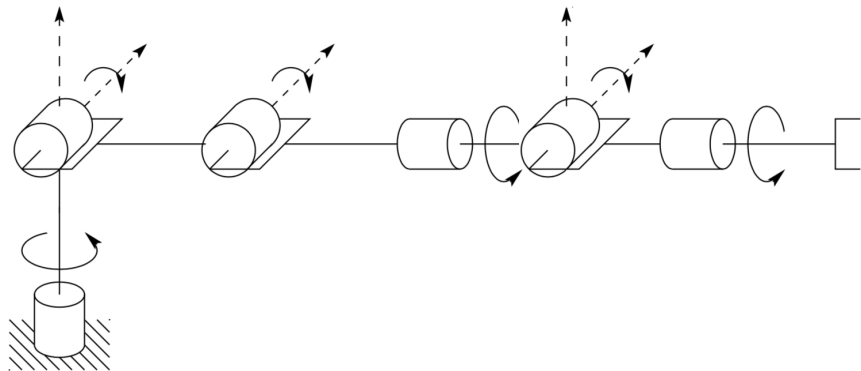


Figure 9: Kinematic Model Representing Zeroed Configuration [1]

4.2.7 The system shall have a removable end effector capable of picking and placing a low-odor chisel tip Expo dry erase marker.

This creates a robot capable of performing a variety of basic tasks, which enhances its educational value.

4.2.7.a The system shall use a parallel gripper that can close to 18mm.

The diameter of a low-odor chisel tip Expo dry erase marker is approximately 18 mm.

4.2.7.b The end effector shall attach to the manipulator using screws configured in a pattern that can accommodate a Dynamixel AX-12A servo.

It is expected that a majority of end effector styles will have to accommodate for a servo to facilitate actuation, therefore a pattern was chosen to standardize the mounting.

4.2.8 The system shall be able to write with a low-odor chisel tip Expo dry erase marker.

4.2.8.a The end effector shall be able to support 0.004 Newton meter moments about the axes normal to its gripping surfaces.

The coefficient of friction between the Expo marker and paper can be approximated and given the weight of an Expo marker the approximate grip strength of the end effector can be calculated.

4.3 Software

The following requirements and specifications are software specific and determine the attributes of the operating system.

4.3.1 The system shall be open source.

This will create an easily obtainable, low cost method of distributing the system's source code, which may be modified for personal use.

4.3.1.a The software shall be hosted publicly on an online repository and maintain an MIT license for distribution.

This allows the end-user to freely download and modify the code without licensing. The MIT license disregards any legal obligation to code upkeep and documentation by the original author.

4.3.2 The system shall be capable of operating given only desired end effector cartesian coordinates specified with respect to the base frame.

4.3.2.a The system shall have a user interface capable of accepting the end-effector's desired cartesian position and Euler angle orientation as a six element row vector.

The system software interface facilitates an untrained user to operate without the advanced knowledge of the system's kinematics.

4.3.2.b The system shall be capable of performing floating point arithmetic.

The solution for the inverse kinematics requires the ability to perform high level arithmetic with little error.

5 Preliminary Design

5.1 CAD

5.1.1 Pulleys

A 12 tooth and 120 tooth pulleys provide a 10:1 gear ratio and use a 0.25 in wide MXL belt. The center distance between the pulleys must be at least 5.43 in to have 5 teeth meshing. Because of the high gear ratio, greater distances do not increase the number of teeth in mesh. Figure AA shows the distance between the manipulator's first two pulleys is 235.185 mm or 9.259 in, which corresponds to a belt with 300 and pitch diameter of 24 in.

Figure BB shows the center distance between the second pulleys is 139.960 mm or 5.510

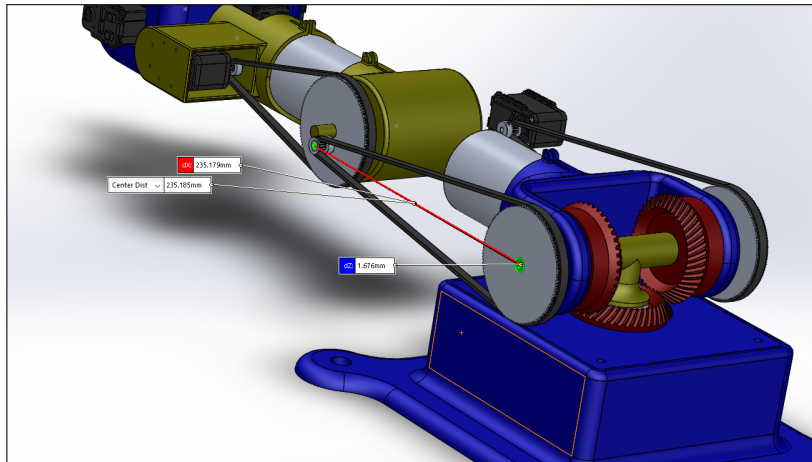


Figure 10: Pulley 1-2 Center Distance

in. The corresponding belt has 208 teeth with a 16.6 in pitch diameter.

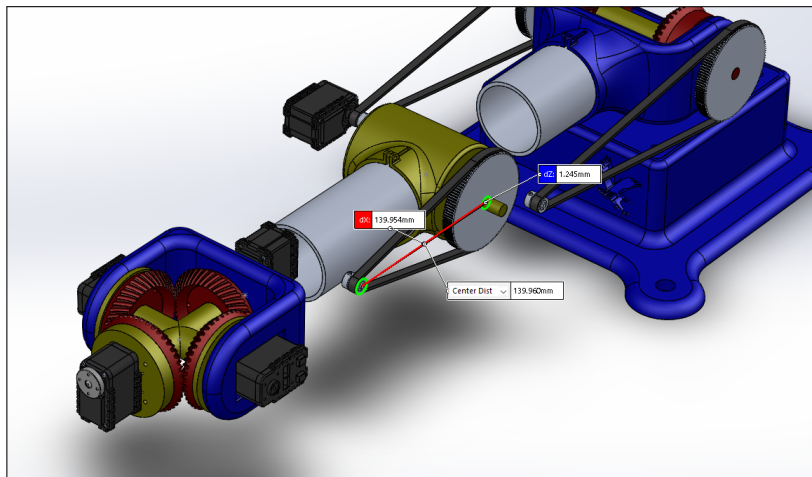


Figure 11: Pulley 3 Center Distance

5.2 Forward Kinematics

The forward kinematics of the manipulator are described by the equations below, where the reference coordinate frames are given by Figure (12).

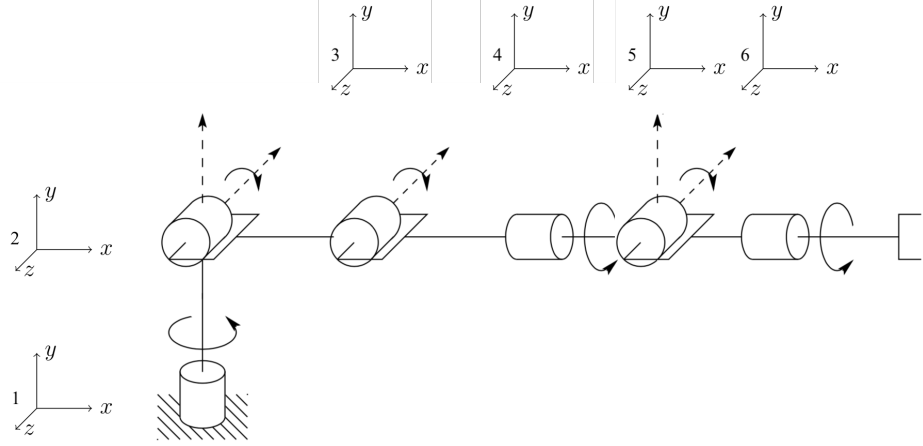


Figure 12: Coordinate Systems

Given the lengths of each of the manipulator links,

$${}^I_B r_1 = \begin{bmatrix} 0 \\ 0 \\ \ell_b \end{bmatrix} \quad {}^1_1 r_2 = \begin{bmatrix} 0 \\ 0 \\ \ell_1 \end{bmatrix} \quad {}^2_2 r_3 = \begin{bmatrix} 0 \\ \ell_2 \\ 0 \end{bmatrix} \quad {}^3_3 r_4 = \begin{bmatrix} 0 \\ \ell_3 \\ 0 \end{bmatrix} \quad {}^4_4 r_5 = \begin{bmatrix} 0 \\ \ell_4 \\ 0 \end{bmatrix} \quad {}^5_5 r_6 = \begin{bmatrix} 0 \\ \ell_5 \\ 0 \end{bmatrix}$$

The position of each link relative to the inertial frame is given as:

$$\begin{aligned} {}^I_B r_1 &= {}_B r_1 & {}^I_B r_2 &= r_1 + {}^I T_{11} {}^1_1 r_2 & {}^I_B r_3 &= r_2 + {}^I T_{22} {}^2_2 r_3 \\ {}^I_B r_4 &= r_3 + {}^I T_{33} {}^3_3 r_4 & {}^I_B r_5 &= r_4 + {}^I T_{44} {}^4_4 r_5 & {}^I_B r_6 &= r_5 + {}^I T_{55} {}^5_5 r_6 \end{aligned}$$

$$\begin{aligned} {}^I_B r_1 &= \begin{bmatrix} 0 \\ 0 \\ \ell_b \end{bmatrix} & {}^I_B r_2 &= \begin{bmatrix} 0 \\ 0 \\ \ell_b + \ell_1 \end{bmatrix} & {}^I_B r_3 &= \begin{bmatrix} -\ell_2 c_{\theta_2} s_{\theta_1} \\ \ell_2 c_{\theta_{12}} \\ \ell_b + \ell_1 + \ell_2 s_{\theta_2} \end{bmatrix} & {}^I_B r_4 &= \begin{bmatrix} -s_{\theta_1} (\ell_3 c_{\theta_{23}} + \ell_2 c_{\theta_2}) \\ c_{\theta_1} (\ell_3 c_{\theta_{23}} + \ell_2 c_{\theta_2}) \\ \ell_1 + \ell_b + \ell_3 s_{\theta_{23}} + \ell_4 s_{\theta_{23}} + \ell_2 s_{\theta_2} \end{bmatrix} \\ {}^I_B r_5 &= \begin{bmatrix} -s_{\theta_1} (\ell_3 c_{\theta_{23}} + \ell_4 c_{\theta_{23}} + \ell_2 c_{\theta_2}) \\ c_{\theta_1} (\ell_3 c_{\theta_{23}} + \ell_4 c_{\theta_{23}} + \ell_2 c_{\theta_2}) \\ \ell_1 + \ell_b + \ell_3 s_{\theta_{23}} + \ell_4 s_{\theta_{23}} + \ell_2 s_{\theta_2} \end{bmatrix} \\ {}^I_B r_6 &= \begin{bmatrix} \ell_5 c_{\theta_1} s_{\theta_4} s_{\theta_5} - \ell_4 c_{\theta_{23}} s_{\theta_1} - \ell_2 c_{\theta_2} s_{\theta_1} - \ell_5 c_{\theta_{23}} c_{\theta_5} s_{\theta_1} - \ell_3 c_{\theta_{23}} s_{\theta_1} \\ + \ell_5 c_{\theta_2} c_{\theta_4} s_{\theta_1} s_{\theta_3} s_{\theta_5} + \ell_5 c_{\theta_3} c_{\theta_4} s_{\theta_1} s_{\theta_2} s_{\theta_5} \\ \ell_5 (s_{\theta_5} (s_{\theta_1} s_{\theta_4} - c_{\theta_4} (c_{\theta_1} c_{\theta_2} s_{\theta_3} + c_{\theta_1} c_{\theta_3} s_{\theta_2})) - c_{\theta_5} (c_{\theta_1} s_{\theta_2} s_{\theta_3} - c_{\theta_1} c_{\theta_2} c_{\theta_3})) \\ - \ell_3 (c_{\theta_1} s_{\theta_2} s_{\theta_3} - c_{\theta_1} c_{\theta_2} c_{\theta_3}) - \ell_4 (c_{\theta_1} s_{\theta_2} s_{\theta_3} - c_{\theta_1} c_{\theta_2} c_{\theta_3}) + \ell_2 c_{\theta_1} c_{\theta_2} \\ \ell_1 + \ell_b + \ell_3 s_{\theta_{23}} + \ell_4 s_{\theta_{23}} + \ell_2 s_{\theta_2} + \frac{\ell_5 c_{\theta_{23}} s_{\theta_{45}}}{2} + \ell_5 s_{\theta_{23}} c_{\theta_5} - \frac{\ell_5 s_{\theta_4 - \theta_5} c_{\theta_{23}}}{2} \end{bmatrix} \end{aligned}$$

Given the direction cosine matrices,

$$rotx(\theta) = \begin{bmatrix} 1 & 0 & 0 \\ 0 & \cos(\theta) & -\sin(\theta) \\ 0 & \sin(\theta) & \cos(\theta) \end{bmatrix}, \quad roty(\theta) = \begin{bmatrix} 1 & 0 & 0 \\ 0 & \cos(\theta) & -\sin(\theta) \\ 0 & \sin(\theta) & \cos(\theta) \end{bmatrix}$$

$$rotz(\theta) = \begin{bmatrix} \cos(\theta) & 0 & \sin(\theta) \\ 0 & 1 & 0 \\ -\sin(\theta) & \cos(\theta) & 0 \end{bmatrix}$$

The orientation of each link with respect to the inertial frame is given as:

$${}^I T_1 = rotz(\theta_1)$$

$${}^I T_2 = rotz(\theta_1) rotx(\theta_2)$$

$${}^I T_3 = rotz(\theta_1) rotx(\theta_2) rotx(\theta_3)$$

$${}^I T_4 = rotz(\theta_1) rotx(\theta_2) rotx(\theta_3) roty(\theta_4)$$

$${}^I T_5 = rotz(\theta_1) rotx(\theta_2) rotx(\theta_3) roty(\theta_4) rotx(\theta_5)$$

$${}^I T_6 = rotz(\theta_1) rotx(\theta_2) rotx(\theta_3) roty(\theta_4) rotx(\theta_5) roty(\theta_6)$$

$${}^I T_1 = \begin{bmatrix} c_{\theta_1} & -s_{\theta_1} & 0 \\ s_{\theta_1} & c_{\theta_1} & 0 \\ 0 & 0 & 1 \end{bmatrix} \quad {}^I T_2 = \begin{bmatrix} c_{\theta_1} & -c_{\theta_2}s_{\theta_1} & s_{\theta_1}s_{\theta_2} \\ s_{\theta_1} & c_{\theta_1}c_{\theta_2} & -c_{\theta_1}s_{\theta_2} \\ 0 & s_{\theta_2} & c_{\theta_2} \end{bmatrix} \quad {}^I T_3 = \begin{bmatrix} c_{\theta_1} & -c_{\theta_{23}}s_{\theta_1} & s_{\theta_{23}}s_{\theta_1} \\ s_{\theta_1} & c_{\theta_{23}}c_{\theta_1} & -s_{\theta_{23}}c_{\theta_1} \\ 0 & s_{\theta_{23}} & c_{\theta_{23}} \end{bmatrix}$$

$${}^I T_4 = \begin{bmatrix} c_{\theta_1}c_{\theta_4} - s_{\theta_{23}}s_{\theta_1}s_{\theta_4} & -c_{\theta_{23}}s_{\theta_1} & c_{\theta_1}s_{\theta_4} + s_{\theta_{23}}c_{\theta_4}s_{\theta_1} \\ c_{\theta_4}s_{\theta_1} + s_{\theta_{23}}c_{\theta_1}s_{\theta_4} & c_{\theta_{23}}c_{\theta_1} & s_{\theta_1}s_{\theta_4} - s_{\theta_{23}}c_{\theta_1}c_{\theta_4} \\ -c_{\theta_{23}}s_{\theta_4} & s_{\theta_{23}} & c_{\theta_{23}}c_{\theta_4} \end{bmatrix}$$

$${}^I T_5 = \begin{bmatrix} c_{\theta_1}c_{\theta_4} - s_{\theta_{23}}s_{\theta_1}s_{\theta_4} & s_{\theta_5}(c_{\theta_1}s_{\theta_4} + s_{\theta_{23}}c_{\theta_4}s_{\theta_1}) - c_{\theta_{23}}c_{\theta_5}s_{\theta_1} & c_{\theta_5}(c_{\theta_1}s_{\theta_4} + s_{\theta_{23}}c_{\theta_4}s_{\theta_1}) + c_{\theta_{23}}s_{\theta_1}s_{\theta_5} \\ c_{\theta_4}s_{\theta_1} + s_{\theta_{23}}c_{\theta_1}s_{\theta_4} & s_{\theta_5}(s_{\theta_1}s_{\theta_4} - s_{\theta_{23}}c_{\theta_1}c_{\theta_4}) + c_{\theta_{23}}c_{\theta_1}c_{\theta_5} & c_{\theta_5}(s_{\theta_1}s_{\theta_4} - s_{\theta_{23}}c_{\theta_1}c_{\theta_4}) - c_{\theta_{23}}c_{\theta_1}s_{\theta_5} \\ -c_{\theta_{23}}s_{\theta_4} & s_{\theta_{23}}c_{\theta_5} + c_{\theta_{23}}c_{\theta_4}s_{\theta_5} & c_{\theta_{23}}c_{\theta_4}c_{\theta_5} - s_{\theta_{23}}s_{\theta_5} \end{bmatrix}$$

$${}^I T_6 = \begin{bmatrix} {}^I T_{6(1,1)} & {}^I T_{6(1,2)} & {}^I T_{6(1,3)} \\ {}^I T_{6(2,1)} & {}^I T_{6(2,2)} & {}^I T_{6(2,3)} \\ {}^I T_{6(3,1)} & {}^I T_{6(3,2)} & {}^I T_{6(3,3)} \end{bmatrix}$$

$${}^I T_{6(1,1)} = c_{\theta_6}(c_{\theta_1}c_{\theta_4} - s_{\theta_{23}}s_{\theta_1}s_{\theta_4}) - s_{\theta_6}(c_{\theta_5}(c_{\theta_1}s_{\theta_4} + s_{\theta_{23}}c_{\theta_4}s_{\theta_1}) + c_{\theta_{23}}s_{\theta_1}s_{\theta_5})$$

$${}^I T_{6(1,2)} = s_{\theta_5}(c_{\theta_1}s_{\theta_4} + s_{\theta_{23}}c_{\theta_4}s_{\theta_1}) - c_{\theta_{23}}c_{\theta_5}s_{\theta_1}$$

$${}^I T_{6(1,3)} = c_{\theta_6}(c_{\theta_5}(c_{\theta_1}s_{\theta_4} + s_{\theta_{23}}c_{\theta_4}s_{\theta_1}) + c_{\theta_{23}}s_{\theta_1}s_{\theta_5}) + s_{\theta_6}(c_{\theta_1}c_{\theta_4} - s_{\theta_{23}}s_{\theta_1}s_{\theta_4})$$

$${}^I T_{6(2,1)} = c_{\theta_6}(c_{\theta_4}s_{\theta_1} + s_{\theta_{23}}c_{\theta_1}s_{\theta_4}) - s_{\theta_6}(c_{\theta_5}(s_{\theta_1}s_{\theta_4} - s_{\theta_{23}}c_{\theta_1}c_{\theta_4}) - c_{\theta_{23}}c_{\theta_1}s_{\theta_5})$$

$${}^I T_{6(2,2)} = s_{\theta_5}(s_{\theta_1}s_{\theta_4} - s_{\theta_{23}}c_{\theta_1}c_{\theta_4}) + c_{\theta_{23}}c_{\theta_1}c_{\theta_5}$$

$${}^I T_{6(2,3)} = s_{\theta_6}(c_{\theta_4}s_{\theta_1} + s_{\theta_{23}}c_{\theta_1}s_{\theta_4}) + c_{\theta_6}(c_{\theta_5}(s_{\theta_1}s_{\theta_4} - s_{\theta_{23}}c_{\theta_1}c_{\theta_4}) - c_{\theta_{23}}c_{\theta_1}s_{\theta_5})$$

$${}^I T_{6(3,1)} = s_{\theta_6}(s_{\theta_{23}}s_{\theta_5} - c_{\theta_{23}}c_{\theta_4}c_{\theta_5}) - c_{\theta_{23}}c_{\theta_6}s_{\theta_5}$$

$${}^I T_{6(3,2)} = s_{\theta_{23}}c_{\theta_5} + c_{\theta_{23}}c_{\theta_4}s_{\theta_5}$$

$${}^I T_{6(3,3)} = c_{\theta_6}(s_{\theta_{23}}s_{\theta_5} - c_{\theta_{23}}c_{\theta_4}c_{\theta_5}) - c_{\theta_{23}}s_{\theta_4}s_{\theta_5}$$

5.3 Velocity Kinematics

The translational and rotational velocities (\dot{r} & ω) can be found given the geometric jacobian of the body and transformation matrix corresponding to it.

$$\begin{bmatrix} {}^B\omega_I \\ {}^I_B\dot{r}_B \end{bmatrix} = J_B = \begin{bmatrix} {}^I T_B(:, 3)^T \cdot \frac{\partial}{\partial \gamma} {}^I T_B(:, 2) \\ {}^I T_B(:, 1)^T \cdot \frac{\partial}{\partial \gamma} {}^I T_B(:, 3) \\ {}^I T_B(:, 2)^T \cdot \frac{\partial}{\partial \gamma} {}^I T_B(:, 1) \end{bmatrix}$$

5.4 Inverse Kinematics

The inverse kinematics can be calculated given desired position and orientation vectors, o and R , respectively.

$$\begin{bmatrix} x_c & y_c & z_c \end{bmatrix} = o, \quad R = \begin{bmatrix} r_{11} & r_{12} & r_{13} \\ r_{21} & r_{22} & r_{23} \\ r_{31} & r_{32} & r_{33} \end{bmatrix}$$

Inverse Position :

$$\begin{aligned} \theta_1 &= \text{atan2}(x_c, y_c) - \pi/2 \\ \theta_2 &= \text{atan2}\left(z_c - \ell_1, \sqrt{x_c^2 + y_c^2}\right) - \text{atan2}(\ell_3 s_3, \ell_2 + \ell_3 c_3) \\ \theta_3 &= \text{atan2}(-\sqrt{1 - D^2}, D) \\ \text{where } D &\equiv \frac{x_c^2 + y_c^2 + (z_c - \ell_1)^2 - \ell_2^2 - \ell_3^2}{2\ell_2\ell_3} \end{aligned}$$

Inverse Orientation :

$$\begin{aligned} {}^I T_3 &= \text{rotz}(\theta_1) \text{rotx}(\theta_2) \text{rotx}(\theta_3) \\ {}^3 T_6 &= {}^I T_3^T R \\ \theta_4 &= \text{atan2}\left({}^3 T_{6(1,2)}, {}^3 T_{6(3,2)}\right) \\ \theta_5 &= \text{atan2}\left({}^3 T_{6(3,2)}/c_4, {}^3 T_{6(2,2)}\right) \\ \theta_6 &= \text{atan2}\left({}^3 T_{6(2,1)}, -{}^3 T_{6(2,3)}\right) \end{aligned}$$

5.5 Equations of Motion

$$H(\gamma)\ddot{\gamma} + d(\gamma, \dot{\gamma}) + G(\gamma) + B(\dot{\gamma}) + C\text{sgn}(\dot{\gamma}) = F \quad (1)$$

$$\overset{B}{\Gamma} = \overset{B}{r}_{cm} m_b , \quad \overset{\circ}{S}(\omega)r = (\omega \times r)$$

$$G(\gamma) \equiv \left(\frac{\partial U(^I r(\gamma))}{\partial \gamma} \right)^T$$

$$U_B = \begin{bmatrix} 0 & 0 & g \end{bmatrix} \left(\overset{I}{r}_B m_B + \overset{I}{T}_B \overset{B}{\Gamma} \right)$$

$$H(\gamma) = \sum_B^N J_B(\gamma)^T \begin{bmatrix} \overset{B}{J} & \overset{\circ}{S}(\overset{B}{\Gamma})^I T_B^T \\ \overset{I}{T}_B \overset{\circ}{S}(\overset{B}{\Gamma})^T & m_B I \end{bmatrix} J_B(\gamma) \quad (2)$$

$$d(\gamma, \dot{\gamma}) = \sum_B^N J_B(\gamma)^T \begin{bmatrix} \overset{B}{J} & \overset{\circ}{S}(\overset{B}{\Gamma})^I T_B^T \\ \overset{I}{T}_B \overset{\circ}{S}(\overset{B}{\Gamma})^T & m_B I \end{bmatrix} \dot{J}_B(\gamma, \dot{\gamma}) \dot{\gamma} + J_B(\gamma)^T \begin{bmatrix} \overset{B}{\omega}_I \times \overset{B}{J}_B \overset{B}{\omega}_I \\ \overset{I}{T}_B \left(\overset{B}{\omega}_I \times (\overset{B}{\omega}_I \times \overset{B}{\Gamma}) \right) \end{bmatrix} \quad (3)$$

5.6 Open-Loop Simulation

5.7 Control System

5.8 Closed-Loop Simulation

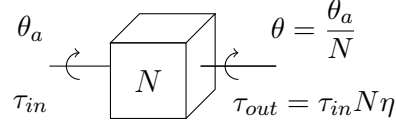
Given robot dynamics described by $H(\gamma)\ddot{\gamma} + n(\gamma, \dot{\gamma}) = \tau$, the torque, τ , provided by the servo motors is necessary to solve the closed loop dynamics of the system. Assuming the servo is driven by a D.C. motor with proportional derivative control,

$$\tau_a = Ki_a = J_a\ddot{\theta}_a + b_a\dot{\theta}_a + \tau_L \quad (4)$$

Where τ_a is the actuator torque, K is the back-EMF constant, i_a is the motor current, J_a is the armature inertia, θ_a , $\dot{\theta}_a$, $\ddot{\theta}_a$ is the motor position and it's first and second time derivatives respectively, b_a is the viscous friction coefficient, and τ_L is the torque available for the actuator to do work. The basic equation for a motor is known to be:

$$V_a = i_a R_a + K\dot{\theta}_a \quad (5)$$

Where V_a is the voltage applied to the actuator and R_a is the armature resistance. Given a gearbox with in/out ratio N and efficiency η ,



The motor equation (4) can be expressed in the output coordinates:

$$Ki_a = J_a N \ddot{\theta} + b_a N \dot{\theta} + \frac{\tau}{N\eta}$$

Substituting into equation (5) and solving for i_a :

$$\begin{aligned} i_a &= \frac{J_a N}{K} \ddot{\theta} + b_a N \dot{\theta} + \frac{\tau}{N\eta} \\ V_a &= \frac{R_a J_a N}{K} \ddot{\theta} + \frac{R_a b_a N}{K} \dot{\theta} + \frac{R_a}{KN\eta} \tau + KN\dot{\theta} \end{aligned} \quad (6)$$

Assuming PD control, $V_a = K_p(\theta - \theta_d) + K_d\dot{\theta}$, where θ_d is the desired orientation of the actuator, the following solution is found by setting the PD solution equal to (6). After collecting like terms:

$$\frac{R_a J_a N}{K} \ddot{\theta} + \left(\frac{R_a J_a N}{K} - K_d + KN \right) \dot{\theta} - K_p \theta = -K_p \theta_d - \frac{R_a}{KN\eta} \tau \quad (7)$$

The following parameters of the system can be obtained by applying a step input to the system with $\tau = 0$ and measuring the characteristics of it's response. Denoting ζ as the damping ratio and ω_n as the natural frequency of the system,

$$\% \text{ Overshoot} = \left(\frac{\theta_{max} - \theta_{ss}}{\theta_{ss}} \right) \times 100 , \quad \zeta = \frac{-\ln(\% \text{OS}/100)}{\sqrt{\pi^2 + \ln^2(\% \text{OS}/100)}} , \quad \omega_n = \frac{\pi}{T_p \sqrt{1 - \zeta^2}}$$

Given θ_{max} , θ_{ss} , and T_p as measured parameters of the system's max output, steady state, and time to peak, respectively.

Refactoring equation (7) and equating with the general solution for a second order system given by $\ddot{\theta} + 2\zeta\omega_n\dot{\theta} + \omega_n^2\theta = \omega_n^2\theta_d$, the following solutions are found:

$$2\zeta\omega_n = \frac{b_a}{J_a} - \frac{KK_d}{R_a J_a N} + \frac{K^2}{R_a J_a} \quad (8) \quad \omega_n^2 = \frac{-KK_p}{R_a J_a N} \quad (9)$$

Performing a similar experiment as previously described, except with a known inertial load $\tau = J_m\ddot{\theta}$, the following parameters can be found:

$$\alpha_m \equiv 2\zeta\omega_n = \frac{R_a b_a N^2 \eta - KK_d N \eta + K^2 N^2 \eta}{R_a J_a N^2 \eta + R_a J_m} , \quad \beta_m \equiv \omega_n = -\frac{KK_p N \eta}{R_a J_a N^2 \eta + R_a J_m}$$

$$\begin{bmatrix} 1 & -(\alpha_1 J_1 + \beta_1 J_1) \\ 1 & -(\alpha_2 J_2 + \beta_2 J_2) \\ \vdots & \vdots \end{bmatrix} \begin{bmatrix} \frac{R_a b_a N^2 \eta - KK_d N \eta + K^2 N^2 \eta - KK_p N \eta}{R_a J_a N^2 \eta} \\ \vdots \\ \frac{1}{J_a N^2 \eta} \end{bmatrix} = \begin{bmatrix} \alpha_1 + \beta_1 \\ \alpha_2 + \beta_2 \\ \vdots \end{bmatrix} \quad (10)$$

With multiple datasets (varying inertial loads, J_m), the solutions of (10) can be found using the least-squares method, yeilding

$$\frac{R_a b_a N - KK_d + K^2 N \eta - KK_p}{R_a J_a N} \quad (11) \quad \frac{1}{J_a N^2 \eta} \quad (12)$$

Finally, the coefficients of the second order system (13) are known:

$$\underbrace{\left(J_a N^2 \eta \right)}_{1/(12)} \ddot{\theta} + \underbrace{\left(\frac{R_a b_a N^2 \eta - KK_d N \eta + K^2 N^2 \eta}{R_a} \right)}_{(8)/(12)} \dot{\theta} - \underbrace{\left(\frac{KK_p N \eta}{R_a} \right)}_{(9)/(12)} \theta + \underbrace{\left(\frac{KK_p N \eta}{R_a} \right)}_{(9)/(12)} \theta_d = -\tau \quad (13)$$

The torque provided by the servo can now be solved for, given the current position (θ), velocity ($\dot{\theta}$), angular acceleration ($\ddot{\theta}$), and desired position (θ_d) are known.

Given the complete equation for the dynamical response of the system (1), substituting in the solution obtained for the motor dynamics and solving for the acceleration,

$$\left(H + J_a N^2 \eta\right)^{-1} \left[\left(B - \frac{R_a b_a N^2 \eta - K K_d N \eta + K^2 N^2 \eta}{R_a} \right) \dot{\gamma} - \left(\frac{K K_p N \eta}{R_a} \right) (\gamma_d - \gamma) - n \right] = \ddot{\gamma} \quad (14)$$

Where

$$n(\gamma, \dot{\gamma}) = d(\gamma, \dot{\gamma}) + G(\gamma) + C \operatorname{sgn}(\dot{\gamma})$$

The closed-loop system can now be simulated, the results are shown below in Figure (13).

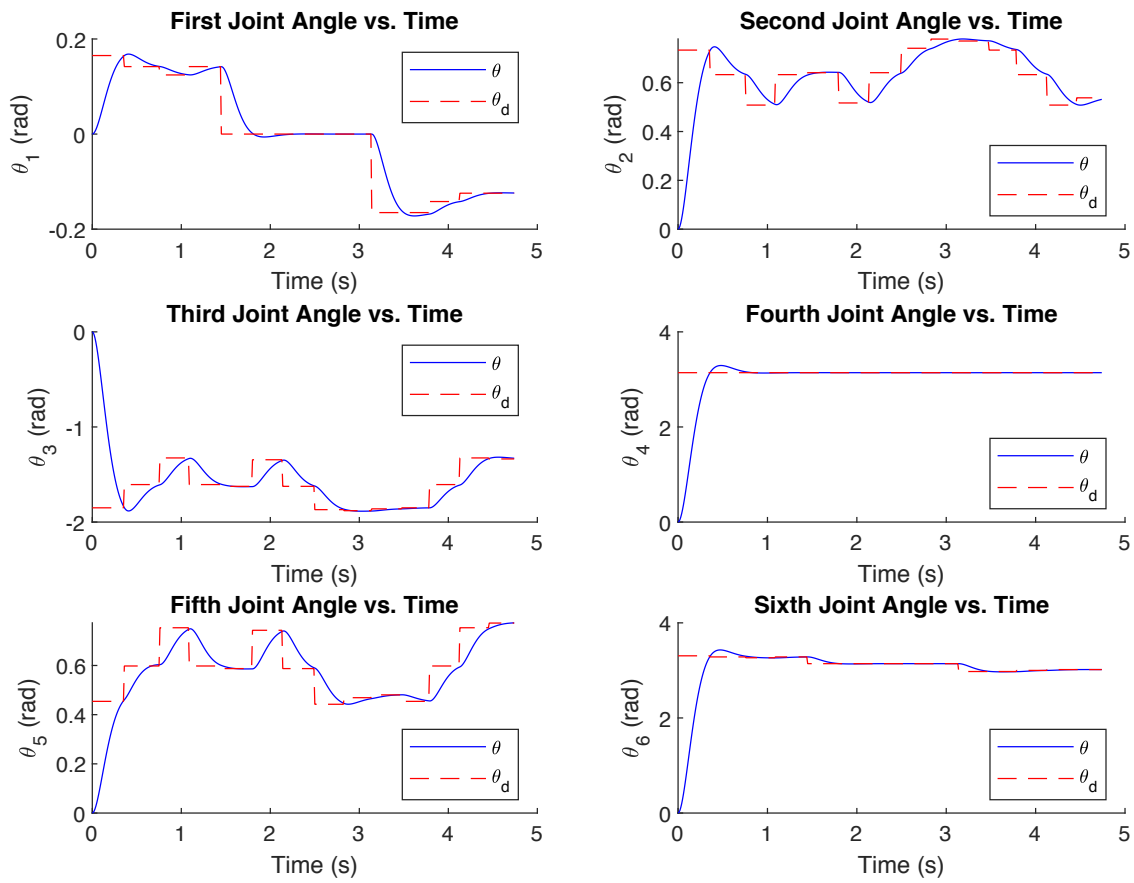


Figure 13: Joint Angles vs Time

5.9 ANSYS

5.10 Electrical Schematic

5.11 Software Flowchart

5.12 Project Status and Future

5.13 Parts List

Acknowledgements & Attributions

We would like to acknowledge the following people for their contributions to creating this report?

— Dr. Isenberg

— Dr. Schipper

I Appendix

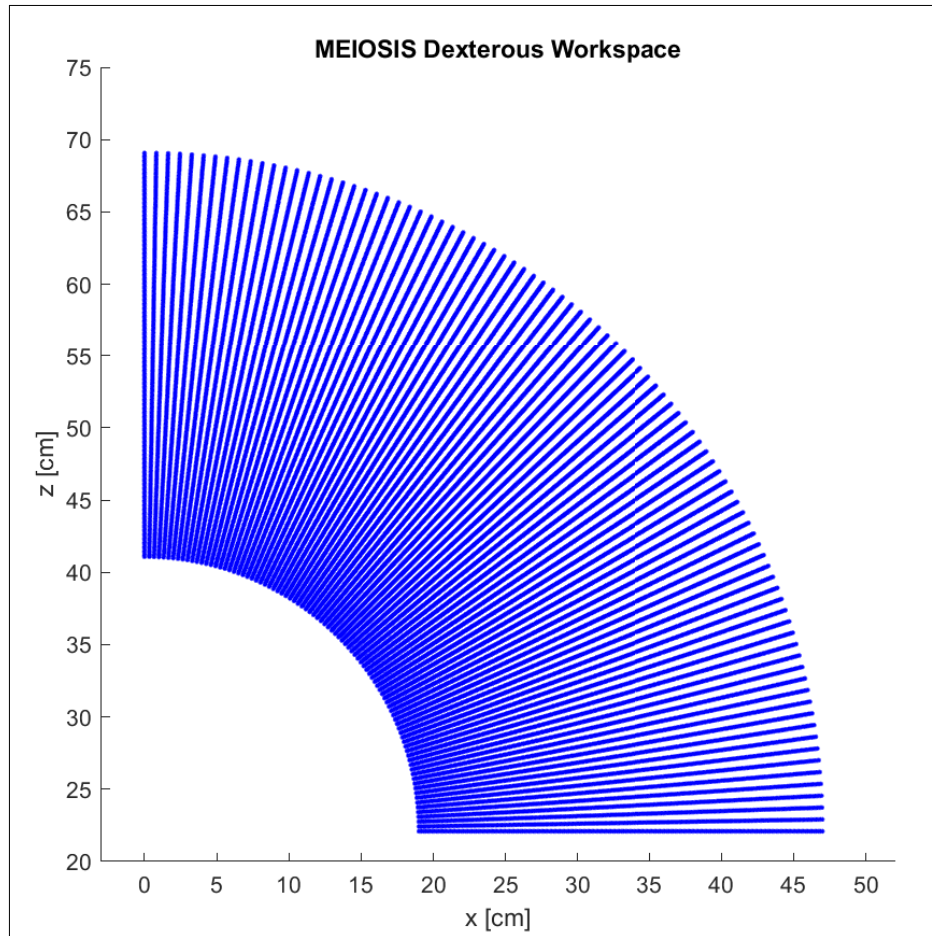


Figure 14: Cross Section of Dexterous Workspace Quadrant

I.i Drawings

I.ii Salient Code

References

- [1] S. Hutchinson M. Spong and M. Vidyasager. *Robot Modeling and Control*. 2006.